Journal of Nuclear Materials 463 (2015) 424–427

Contents lists available at ScienceDirect

Journal of Nuclear Materials

journal homepage: www.elsevier.com/locate/jnucmat

Investigation of SOL parameters and divertor particle flux from electric probe measurements in KSTAR

J.G. Bak [a,*,1], H.S. Kim [a], M.K. Bae [b], J.W. Juhn [a], D.C. Seo [a], E.N. Bang [a], S.B. Shim [c], K.S. Chung [b], H.J. Lee [c], S.H. Hong [a]

[a] National Fusion Research Institute, Daejeon, Republic of Korea
[b] Hanyang University, Seoul, Republic of Korea
[c] Pusan National University, Pusan, Republic of Korea

ARTICLE INFO

Article history:
Available online 26 November 2014

ABSTRACT

The upstream scrape-off layer (SOL) profiles and downstream particle fluxes are measured with a fast reciprocating Langmuir probe assembly (FRLPA) at the outboard mid-plane and a fixed edge Langmuir probe array (ELPA) at divertor region, respectively in the KSTAR. It is found that the SOL has a two-layer structure in the outboard wall-limited (OWL) ohmic and L-mode: a near SOL (~5 mm zone) with a narrow feature and a far SOL with a broader profile. The near SOL width evaluated from the SOL profiles in the OWL plasmas is comparable to the scaling for the L-mode divertor plasmas in the JET and AUG. In the SOL profiles and the divertor particle flux profile during the ELMy H-modes, the characteristic e-folding lengths of electron temperature, plasma density and particle flux during an ELM phase are about two times larger than ones at the inter ELM.

1. Introduction

The steady state power load at the divertor target should be less than 10 MW m^{-2} [1] due to the thermal engineering limitation in the material of the divertor target, which is a critical design parameter in the next step device such as ITER. The scrape-off layer (SOL) width λ_q is an important quantity that is directly related to the divertor heat flux q_{div}, as the power load at the divertor target, for the heating power during a discharge in the magnetic confinement device. The SOL width has been calculated by using the upstream SOL plasma parameters such as e-folding lengths of electron temperature T_e and plasma density n_e at the outboard mid-plane (OMP) [2] or evaluated from the divertor heat flux profile mapped to the OMP [3].

Up to now, the radial profiles of T_e and n_e were measured by using a fast reciprocating Langmuir probe assembly (FRLPA) with a maximum speed of 1.5 m/s in the SOL region at the OMP and the ion saturation currents were measured with the fixed edge Langmuir probe array (ELPA) at the divertor region in order to study the characteristics of the SOL and divertor plasmas in the KSTAR [4]. After the H-mode plasma was routinely produced in the KSTAR, the investigations of the SOL width and divertor heat flux were needed to evaluate the power load on the divertor target in the H-mode plasmas because the heating power has been gradually increased for high plasma performance in the KSTAR. Thus, the initial evaluation of the SOL width and divertor particle flux from the electric probe measurements were carried out for the study of power load on the divertor target in the KSTAR.

In this work, the results from the preliminary investigation of the SOL parameters and divertor particle flux during ohmic, L-mode and H-mode discharges in the KSTAR are presented.

2. Characteristic e-folding lengths and SOL width at the upstream in the outboard wall limited plasmas

The SOL profiles of electron temperature T_e and plasma density n_e were obtained from the FRLPA [4] measurements at the OMP in the outboard wall limiter (OWL) magnetic configuration during ohmic and L-mode discharges in the KSTAR. It was found that there was a two-layer structure in the SOL region for the OWL configuration: a steep gradient within ~5 mm near the last closed flux surface (LCFS) and a slow decay at far SOL as observed for the divertor plasmas in the Alcator C-Mod [5]. The near and far SOL regions are usually separated at about 2–3 characteristic SOL power width from the separatrix at the OMP [6]. The radial profiles in the two regions are determined by parallel and perpendicular transports, together with the heat and particle sources; particle transport in

* Corresponding author at: 169-148 Gwahangno, Yuseong-gu, Daejeon 305-806, Republic of Korea.
E-mail address: jgbak@nfri.re.kr (J.G. Bak).
[1] Presenting author.

http://dx.doi.org/10.1016/j.jnucmat.2014.11.075
0022-3115/

the near SOL exhibits a strong scaling with collisionality, while transport in the far SOL is clearly convective, with little obvious dependence on collisionality [7]. These two-zone SOL structures have been observed on most tokamaks [7]. Thus, exponential fits on the radial profiles in two regions were separately carried out by using a simple exponential function as $f(x) \propto \exp(-x/\lambda)$. The upstream SOL width λ_q was evaluated from the relation in the flux limited regime with low collisionality as $\lambda_q \approx \{[(3/2)/\lambda_{T_e}]+(1/\lambda_{n_e})\}^{-1}$ [8] by using characteristic e-folding lengths λ_{T_e}, λ_{n_e} obtained from the SOL profiles. Here, it was assumed that $T_e \sim T_i$ because T_i was not able to be measured at the OMP region. It was noted that the value of T_i/T_e increased up to 11 at the far SOL region [6], thus, far SOL λ_q was evaluated by using the relation as $\lambda_q \approx [(1/\lambda_{T_e})+(1/\lambda_{n_e})]^{-1}$ [9].

Fig. 1(a)–(b) shows typical radial profiles of n_e and T_e with sharp and broad widths in the OWL configuration during an ohmic discharge, respectively. The value of $\lambda_{T_e}(\lambda_{n_e})$ at near SOL (within 5 mm outside the LCFS) and at far SOL (in the outside region of the poloidal limiter) are 4.18 (3.36) mm and 46.7 (24.8) mm, respectively. The ratios of $\lambda_{T_e}/\lambda_{n_e}$ were 1.25 and 1.88 near and far SOLs, respectively. Thus, the narrow SOL width and the far SOL width are evaluated as 1.5 mm and as 13.8 mm, respectively. The sharp feature near the SOL is also observed in the radial profile of the parallel SOL velocity measured with Mach probe as shown in Fig. 1(c). The position of the LCFS during the radial profile measurement was checked by using plasma shape reconstructed from the equilibrium and reconstruction fitting code (EFIT). Fig. 1(d) shows a typical plasma shape reconstructed from the EFIT at a certain time. Here, experimental conditions were as following: toroidal magnetic field on axis, $B_T = 2.0$ T; plasma current, $I_p = 0.42$ MA; line averaged density, $n_e = 2.2 \times 10^{19}$ m^{-3}; safety factor at the 95% flux surface, $q_{95} = 4.6$; ohmic power, $P_{OH} = 0.28$ MW; plasma elongation, $\kappa = 1.4$.

For the OWL ohmic and L-mode plasmas, there is good linear relation between λ_{T_e} and λ_{n_e} for near SOL and far SOL as $\lambda_{T_e} \approx 1.1\lambda_{n_e}$, $\lambda_{T_e} \approx 1.2\lambda_{n_e}$, respectively as shown in Fig. 2(a). The value of $(\lambda_{T_e}/\lambda_{n_e})$ in the far SOL region was slightly higher than near SOL value. It might be expected that the energy and particle diffusivities in the two regions could be similar by considering that $(\lambda_{T_e}/\lambda_{n_e})$ is a function of the cross-field electron heat-to-particle diffusivity ratio $(\chi_\perp^e/D_\perp)$ obtained from particle and energy balances in the simple SOL model [9]. There are two assumptions to get the relation between $(\lambda_{T_e}/\lambda_{n_e})$ and $(\chi_\perp^e/D_\perp)$; both cross-field convection and conduction contribute to the electron power flow into the SOL, and the cross-field conduction is anomalous [9]. In addition, the narrow SOL width $\lambda_{q,meas}$ is comparable to the scaling of λ_q as shown in Fig. 2(b). The scaling was evaluated for the L-mode divertor phases in the JET and AUG as λ_q[mm] = 1.44 $B_T^{-0.8}$[T] $q_{95}^{1.14}$ $P_{SOL}^{0.22}$[MW] $R_0^{0.03}$[m] [10]. The far SOL widths $\lambda_{q,meas}$ are scattered, and the averaged value of $\lambda_{q,meas}$ is about ten times larger than one in near SOL region. Here, total heating power (ohmic plus neutral beam (NB) power) P_{TOT} is 0.28–0.34 and 1.55 MW, and power crossing the separatrix into the SOL P_{SOL} is 0.2–0.23 and 1.1 MW. P_{SOL} is defined as $P_{SOL} = P_{TOT} - dW_{tot}/dt - P_{rad}$ where dW_{tot}/dt is the time rate of change of plasma stored energy, and P_{rad} is the core radiated power (assumed as ~30% of P_{TOT}).

3. Characteristic e-folding lengths at the upstream in ELMy H-mode plasmas

In the ELMy H-mode discharges, the radial profiles of T_e and n_e with several spikes due to ELM bursts during the FRLPA

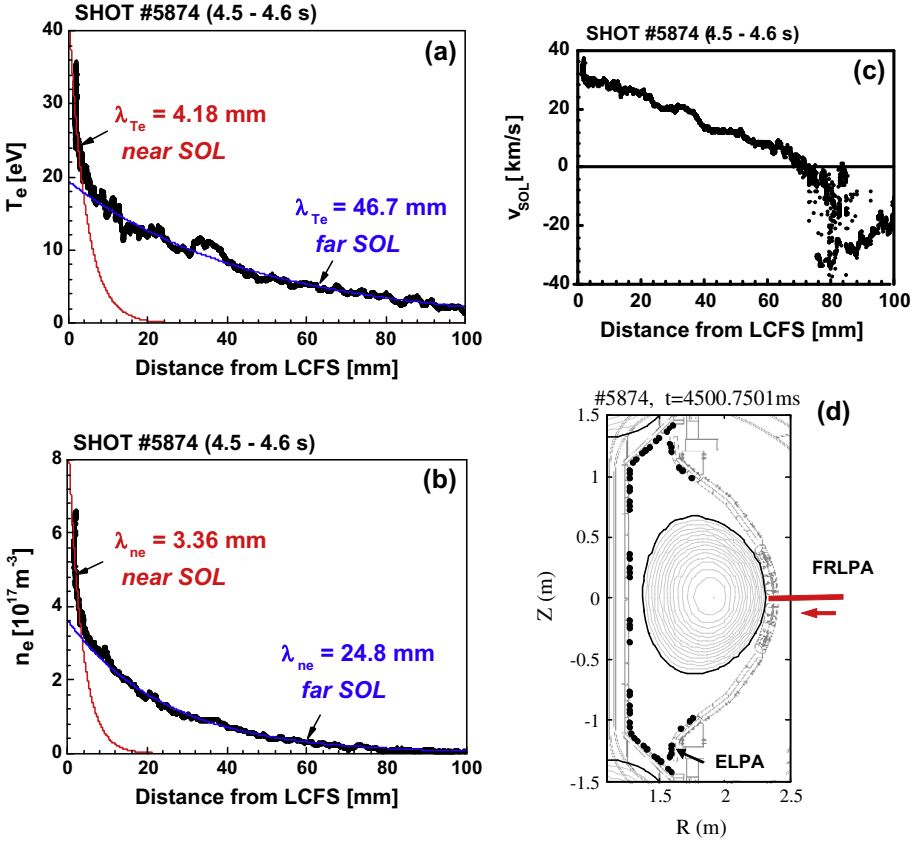

Fig. 1. SOL profiles of plasma parameters measured with the FRLPA and plasma shape with the FRLPA and ELPA in the OWL configuration during an ohmic discharge: (a) electron temperature, (b) plasma density, (c) parallel flow velocity and (d) elongated plasma shape reconstructed from the EFIT a certain time. Here, the location of the LCFS has the uncertainty of about 1 cm.

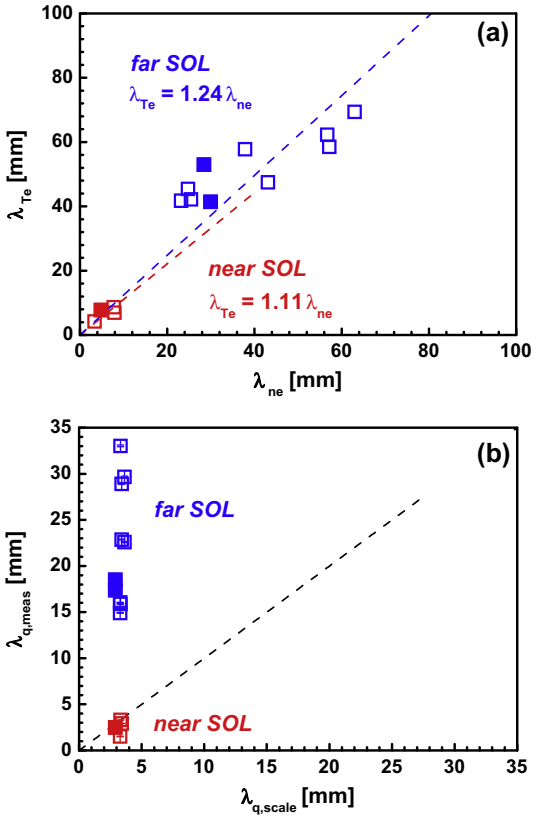

Fig. 2. Characteristics of the SOL in the OWL configuration during ohmic and L-mode discharges (B_T = 2.0 T, I_p = 0.4–0.6 MA, n_e = 1.9–4.0 × 10^{19} m^{-3}, q_{95} = 3.0–5.0, κ = 1.2–1.4): (a) relation between characteristic e-folding lengths, λ_{T_e} vs. λ_{n_e} for near and far SOLs and (b) the measured SOL width vs. the scaling from JET and AUG (See Eq. (6) in Ref. [10]) for the divertor configuration and the dot line represents $\lambda_{q,meas} = \lambda_{q,scale}$ for near SOL. Here, filled symbols mean L-mode.

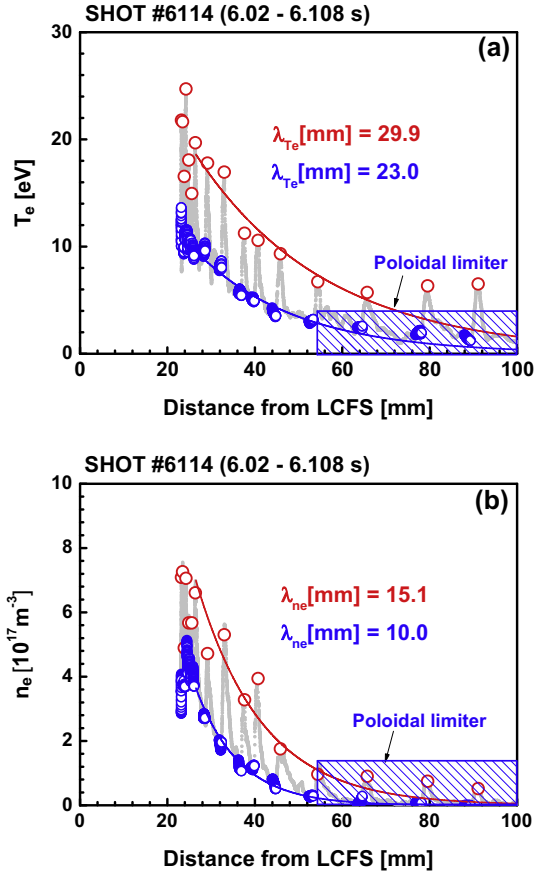

Fig. 3. Radial profiles of plasma parameters measured with the FRLPA during an ELMy H-mode discharge (B_T = 2.0 T, I_p = 0.52 MA, n_e = 2.7 × 10^{19} m^{-3}, q_{95} = 3.4, P_{TOT} = 1.47 MW, κ = 1.83): (a) electron temperature and (b) plasma density. Here box (from 54 mm to 100 mm) means the poloial limiter at the OMP.

measurement are obtained as shown in Fig. 3. The gap distance between the LCFS and the poloidal limiter was less than 60 mm. The ELM frequency was about 200 Hz, which might corresponded to the type-III ELM by considering the total heating power of less than 1.5 MW during the discharge. The radial profiles from the FRLPA measurement were able to be obtained up to 20 mm outside the LCFS during H-mode discharges. Thus, it was thought that the characteristic e-folding lengths obtained from the measurement corresponded to the values in far SOL. The e-folding lengths during ELM bursts and inter-ELMs were evaluated from the radial profiles obtained by selecting one data point near each ELM peak and by using 100 data points before each ELM, respectively. Here, 100 data points corresponded to a time difference of 1 ms because the sampling rate in the digitizer for electric probe diagnostic system was 100 kHz. It is found that the e-folding lengths during ELM bursts (λ_{T_e} = 29.9 mm, λ_{n_e} = 15.1 mm) are broader than ones between ELMs (λ_{T_e} = 23.0 mm, λ_{n_e} = 10.0 mm) as shown in Fig. 3, which is similar to the result reported in JET [11]. The values of ($\lambda_{T_e}/\lambda_{n_e}$) were 1.98 and 2.30 for ELM and inter-ELM phases during the H-mode discharge, respectively. It might be expected that cross-field heat transport could be slightly lower than the particle transport during an ELM phase by comparing with the steady state case from the relation between ($\lambda_{T_e}/\lambda_{n_e}$) and ($\chi^e_\perp/D_\perp$) [9] .

4. Divertor particle flux in the ELMy H-mode

The divertor particle flux Γ_{div} was evaluated by using the relation of $\Gamma_{div} = j_{is}/e \sin\alpha$ from ion saturation current density j_{is} measured by each single probe in the fixed ELPA at the divertor region. Where α is the grazing angle between a divertor target surface and an incident magnetic field, which was calculated by using two-estimated angles; an angle between the target surface and the incident poloidal magnetic field, and a pitch angle between poloidal and toroidal magnetic fields. The value of α was assumed as 5°, the value near a strike point, in the evaluation of Γ_{div} because it was difficult to get the exact angles for all over divertor in this work. The particle flux profile from the ELPA measurement had low spatial resolution because of large radial distance between two adjacent divertor probes in the ELPA (up to 8.0 cm). Thus, it was noted that the e-folding length $\lambda_{\Gamma div}$ was able to be evaluated from the profile in some lower single null (LSN) configurations during ELMy H-modes although it was difficult to know the exact peak flux and to evaluate the spreading factor of the particle flux in the private region in this work.

For the investigation of particle flux in the LSN configuration during an ELMy H-mode discharge ($dr_{sep} \approx -0.06$ m, $\kappa \approx 1.89$), an ELM peak is selected as shown in Fig. 4(a). The decrease of the stored energy due to the ELM burst is $\Delta W_{ELM}/W_{tot}$ = ~6% and the ELM frequency is about 44 Hz. Here, Ip = 0.5 MA, B_T = 2.3 T, q_{95} = 7.3, n_e = ~2.4 × 10^{19} m^{-3} and P_{NB} = ~2.67 MW. The maximum particle flux during the ELM burst is more than three time larger than ones before and after the ELM, and the characteristic e-folding length $\lambda_{\Gamma div}$ at the ELM phase is about two times of ones at inter-ELM phases as shown in Fig. 4(b). Here, 1 ms and 0.5 ms time-averaged values were used to get the profiles for inter and during ELM periods, respectively. The longer e-folding length during the ELM was similar to the experimental result reported in the EAST [12].

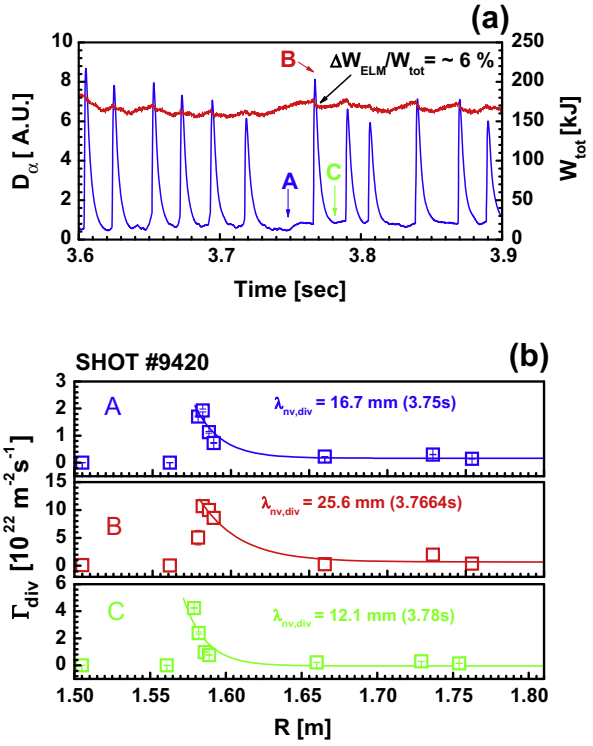

Fig. 4. Divertor particle flux profiles from ELPA measurements in an ELMy H-mode discharge: (a) D_α and W_{tot} signals and (b) flux profiles before, during and after an ELM burst. Here, A, B and C means times before, during and after the ELM burst, respectively.

5. Summary

In the evaluation of upstream SOL width λ_q using characteristic e-folding lengths λ_{T_e} and λ_{n_e} obtained from the FRLPA measurements at the OMP in the OWL ohmic and L-mode plasmas, it was found that the SOL had a two-layer structure: a narrow feature near the LCFS (within 5 mm) and a broad width at far SOL region corresponding to the outside of the poloidal limiter. The value of λ_q at near SOL was slightly lower than the scaling for diverted L-mode plasmas in the JET and AUG. From the FRLPA and ELPA measurements at the upstream SOL and the divertor regions, respectively in the diverted ELMy H-modes, it was investigated that both the values of λ_{T_e} (λ_{n_e}) and $\lambda_{\Gamma div}$ in the ELM phase were about two times larger than ones in the inter-ELM phase although the spatial resolution of the ELPA was not enough to detect an exact peak value in the divertor flux profile.

The evaluation of the SOL width in the inner-wall limited (IWL) plasmas is needed to compare with one for OWL plasmas for clearly understanding the SOL characteristics of the limited plasmas in the KSTAR, together with further study of magnetic connection length and particle/energy transport across the LCFS in the limiter plasmas. In addition, further measurements of the upstream SOL width using the FRLPA during ELMy H-mode discharges are required for study of particle and heat transports in the near and far SOL regions. The measurement of the power load on divertor target by using the infrared camera with the high spatial resolution and the divertor heat flux measurement by modifying the probe configuration from single to triple in the ELPA with more probes, together with the validation of grazing angles for all over divertor, are required for the evalution of the SOL width and the divertor power spreading factor S at the divertor. The divertor flux measurements will be benchmarked by using the scrape-off layer plasma simulation (SOLPS) code to validate the upstream SOL width more accurately and to understand the relation of upstream characteristic e-folding and divertor heat flux as the downstream power load on the divertor target.

Acknowledgements

This work was supported by Korea Ministry of Science, ICT and Future Planning under the KSTAR project contract, and was partly supported by Korea Research Council of Fundamental Science and Technology (KRCF) under the international collaboration & research in Asian countries.

References

[1] J. Linke, Trans. Fusion Sci. Technol. 49 (2006) 455.
[2] D.L. Rudakov et al., J. Nucl. Mater. 415 (2011) S387.
[3] A. Loarte et al., J. Nucl. Mater. 266–269 (1999) 587.
[4] J.G. Bak et al., Contrib. Plasma Phys. 53 (2013) 69.
[5] B. LaBombard et al., J. Nucl. Mater. 415 (2011) S349.
[6] M. Kocan et al., J. Nucl. Mater. 415 (2011) S1133.
[7] J.L. Terry et al., Fusion Sci. Technol. 51 (2007) 342.
[8] P.C. Stangeby et al., Nucl. Fusion 50 (2010) 125003.
[9] P.C. Stangeby, The Plasma Boundary of Magnetic Fusion Devices, Taylor & Francis Group, New York, 2000.
[10] A. Scarabosio et al., J. Nucl. Mater. 438 (2013) S426.
[11] D.N. Hill, J. Nucl. Mater. 241–243 (1997) 182.
[12] L. Wang et al., Nucl. Fusion 52 (2012) 063024.